Article

# Systematic Functionalization of a Metal#Organic Framework via a Postsynthetic Modification Approach

Kristine K. Tanabe, Zhenqiang Wang, and Seth M. Cohen

*J. Am. Chem. Soc.*, **2008**, 130 (26), 8508-8517 • DOI: 10.1021/ja801848j • Publication Date (Web): 10 June 2008



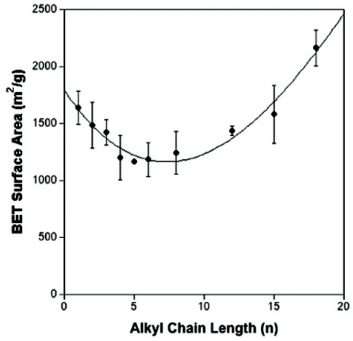


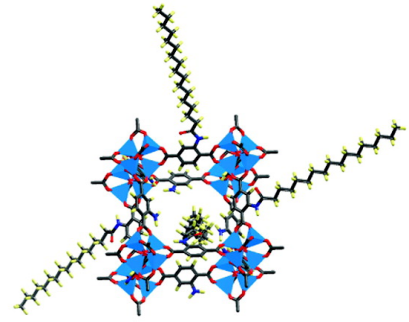

## More About This Article

Additional resources and features associated with this article are available within the HTML version:

- Supporting Information
- Links to the 8 articles that cite this article, as of the time of this article download
- Access to high resolution figures
- Links to articles and content related to this article
- Copyright permission to reproduce figures and/or text from this article

View the Full Text HTML

J|A|C|S
ARTICLES

Published on Web 06/10/2008

# Systematic Functionalization of a Metal−Organic Framework via a Postsynthetic Modification Approach

Kristine K. Tanabe, Zhenqiang Wang, and Seth M. Cohen*

*Department of Chemistry and Biochemistry, University of California, San Diego, 9500 Gilman Drive, La Jolla, California 92093-0358*

Received March 14, 2008; E-mail: scohen@ucsd.edu.

***Abstract:*** The pendant amino groups in isoreticular metal−organic framework-3 (IRMOF-3) were subjected to postsynthetic modification with 10 linear alkyl anhydrides $(O(CO(CH_2)_nCH_3)_2$ (where $n = 1$ to 18) and the extent of conversion, thermal and structural stability, and Brunauer-Emmett-Teller (BET) surface areas of the resulting materials were probed. $^1$H NMR of digested samples showed that longer alkyl chain anhydrides resulted in lower conversions of IRMOF-3 to the corresponding amide framework (designated as IRMOF-3-AM2 to IRMOF-3-AM19). Percent conversions ranged from essentially quantitative (∼99%, -AM2) to ∼7% (-AM19) with IRMOF-3 samples. Modified samples were thermally stable up to approximately 430 °C and remained crystalline based on powder X-ray diffraction (PXRD) measurements. Under specific reaction conditions, significant conversions were obtained with complete retention of crystallinity, as verified by single-crystal X-ray diffraction experiments. Single crystals of modified IRMOF-3 samples all showed that the *F*-centered cubic framework was preserved. All single crystals used for X-ray diffraction were analyzed by electrospray ionization mass spectrometry (ESI-MS) to confirm that these frameworks contained the modified 1,4-benzenedicarboxylate ligand. Single crystals of each modified IRMOF-3 were further characterized by measuring the dinitrogen gas sorption of each framework to determine the effects of modification on the porosity of the MOF. BET surface areas ($m^2$/g) confirmed that all modified IRMOF-3 samples maintained microporosity regardless of the extent of modification. The surface area of modified MOFs was found to correlate to the size and number of substituents added to the framework.

## Introduction

Metal−organic frameworks (MOFs) are crystalline materials generated using metal ions or metal ion clusters that act as "nodes" combined with mulitdentate organic ligands to serve as "rods".[1–16] The use of various metals (nodes) and ligands (rods) under a wide variety of reaction conditions has produced diverse MOF structures that have shown great promise in a range of applications.[12,17–29] In particular, over the past several years, MOFs have increasingly gained popularity as a gas sorption medium due to their high porosity and thermal stability.[30–38]

(1) Hoskins, B. F.; Robson, R. *J. Am. Chem. Soc.* **1989**, *111*, 5962–5964.
(2) Hoskins, B. F.; Robson, R. *J. Am. Chem. Soc.* **1990**, *112*, 1546–1554.
(3) Gardner, G. B.; Venkataraman, D.; Moore, J. S.; Lee, S. *Nature* **1995**, *374*, 792–795.
(4) Yaghi, O. M.; Li, H. L.; Davis, C.; Richardson, D.; Groy, T. L. *Acc. Chem. Res.* **1998**, *31*, 474–484.
(5) Kitagawa, S.; Kondo, M. *Bull. Chem. Soc. Jpn.* **1998**, *71*, 1739–1753.
(6) Robson, R. *J. Chem. Soc., Dalton Trans.* **2000**, 3735–3744.
(7) Eddaoudi, M.; Moler, D. B.; Li, H.; Chen, B.; Reineke, T. M.; O'Keeffe, M.; Yaghi, O. M. *Acc. Chem. Res.* **2001**, *34*, 319–330.
(8) Moulton, B.; Zaworotko, M. J. *Chem. Rev.* **2001**, *101*, 1629–1658.
(9) Janiak, C. *Dalton Trans.* **2003**, 2781–2804.
(10) James, S. L. *Chem. Soc. Rev.* **2003**, *32*, 276–288.
(11) Yaghi, O. M.; O'Keeffe, M.; Ockwig, N. W.; Chae, H. K.; Eddaoudi, M.; Kim, J. *Nature* **2003**, *423*, 705–714.
(12) Kitagawa, S.; Kitaura, R.; Noro, S.-i. *Angew. Chem., Int. Ed.* **2004**, *43*, 2334–2375.
(13) Rao, C. N. R.; Natarajan, S.; Vaidhyanathan, R. *Angew. Chem., Int. Ed.* **2004**, *43*, 1466–1496.
(14) Ockwig, N. W.; Delgado-Friedrichs, O.; O'Keeffe, M.; Yaghi, O. M. *Acc. Chem. Res.* **2005**, *38*, 176–182.
(15) Férey, G.; Mellot-Draznieks, C.; Serre, C.; Millange, F. *Acc. Chem. Res.* **2005**, *38*, 217–225.
(16) Bradshaw, D.; Claridge, J. B.; Cussen, E. J.; Prior, T. J.; Rosseinsky, M. J. *Acc. Chem. Res.* **2005**, *38*, 273–282.
(17) Fujita, M.; Kwon, Y. J.; Washizu, S.; Ogura, K. *J. Am. Chem. Soc.* **1994**, *116*, 1151–1152.
(18) Li, H.; Eddaoudi, M.; O'Keeffe, M.; Yaghi, O. M. *Nature* **1999**, *402*, 276–279.
(19) Chui, S. S.-Y.; Lo, S. M.-F.; Charmant, J. P. H.; Orpen, A. G.; Williams, I. D. *Science* **1999**, *283*, 1148–1150.
(20) Seo, J. S.; Whang, D.; Lee, H.; Jun, S. I.; Oh, J.; Jeon, Y. J.; Kim, K. *Nature* **2000**, *404*, 982–986.
(21) Halder, G. J.; Kepert, C. J.; Moubaraki, B.; Murray, K. S.; Cashion, J. D. *Science* **2002**, *298*, 1762–1765.
(22) Chae, H. K.; Siberio-Perez, D. Y.; Kim, J.; Go, Y.; Eddaoudi, M.; Matzger, A. J.; O'Keeffe, M.; Yaghi, O. M. *Nature* **2004**, *427*, 523–527.
(23) Férey, G.; Mellot-Draznieks, C.; Serre, C.; Millange, F.; Dutour, J.; Surblé, S.; Margiolaki, I. *Science* **2005**, *309*, 2040–2042.
(24) Evans, O. R.; Lin, W. B. *Acc. Chem. Res.* **2002**, *35*, 511–522.
(25) Wu, C. D.; Hu, A.; Zhang, L.; Lin, W. *J. Am. Chem. Soc.* **2005**, *127*, 8940–8941.
(26) Lin, W. B. *J. Solid State Chem.* **2005**, *178*, 2486–2490.
(27) Cho, S.-H.; Ma, B.; Nguyen, S. T.; Hupp, J. T.; Albrecht-Schmitt, T. E. *Chem. Commun.* **2006**, 2563–2565.
(28) Nuzhdin, A. L.; Dybtsev, D. N.; Bryliakov, K. P.; Talsi, E. P.; Fedin, V. P. *J. Am. Chem. Soc.* **2007**, *129*, 12958–12959.
(29) Mueller, U.; Schubert, M.; Teich, F.; Puetter, H.; Schierle-Arndt, K.; Pastré, J. *J. Mater. Chem.* **2006**, *16*, 626–636.
(30) Rosi, N. L.; Eckert, J.; Eddaoudi, M.; Vodak, D. T.; Kim, J.; O'Keeffe, M.; Yaghi, O. M. *Science* **2003**, *300*, 1127–1129.
(31) Férey, G.; Latroche, M.; Serre, C.; Millange, F.; Loiseau, T.; Percheron-Guégan, A. *Chem. Commun.* **2003**, 2976–2977.
(32) Rowsell, J. L. C.; Millward, A. R.; Park, K. S.; Yaghi, O. M. *J. Am. Chem. Soc.* **2004**, *126*, 5666–5667.


**10.1021/ja801848j CCC: $40.75** 

Despite impressive progress in the area of MOFs, it remains a significant challenge to introduce, in a rational and systematic way, more complex functionality within the lattice. Some MOFs with pendant functional groups preinstalled on the organic components have been described, and judicious choice of metal ions in combination with appropriate ligands has allowed for the introduction of metal chromophores or unsaturated metal centers as a means to "functionalize" MOFs.[39–47] The majority of MOFs are formed via solvothermal reactions that typically employ high temperatures and elevated pressures, thereby limiting the possible functional groups that can be directly introduced into the MOF. Cross-reactivity (e.g., the ability to coordinate metal ions or otherwise interfere with formation of the MOF), as well as steric and polarity considerations, further limits the types of substituents that may be incorporated via the solvothermal process.

In a seminal paper on MOFs by Robson et al. in 1990,[2] an intriguing suggestion was made that, "Relatively unimpeded migration of species throughout the lattice may allow chemical functionalization of the rods subsequent to construction of the framework." Stated simply, it should be possible to modify an MOF using small chemical reagents *after* the lattice is formed. A viable route to "postsynthetic" modification of MOFs could provide a general method for introducing functional groups into these materials, generating a greater range of physical and chemical properties than could be achieved by direct synthesis alone. This concept has been applied to materials other than MOFs, and examples include the sulfonation of organosilicates[48,49] and carboxylation, activation, and amide coupling of carbon nanotubes.[50] Despite almost 18 years since Robson's proposal, there are very few reports on postsynthetic modification for MOFs.[20,25,51–59] In a rare example, a crystalline homochiral framework termed POST-1 synthesized by Kim et al.[20] from a pyridine derivative of D-tartaric acid and zinc(II) was modified in a postsynthetic fashion. It was shown that the free pyridyl groups present in the cavities of POST-1 could undergo *N*-alkylation using an excess of iodomethane or iodohexane at room temperature. Evidence was also provided that indicated POST-1 remained structurally intact after postsynthetic modification.

In a recent study, we demonstrated that isoreticular metal−organic framework-3 (IRMOF-3) can be postsynthetically modified under mild conditions, undergoing a single-crystal-to-single-crystal transformation.[59] IRMOF-3 is a rigid cubic framework comprised of $Zn_4O$ secondary building unit (SBU) nodes and 2-aminobenzenedicarboxylate ($NH_2$−BDC) rods. IRMOF-3 was selected due to its highly porous, crystalline structure and the presence of noncoordinating amino groups on the benzenedicarboxylate (BDC) linker,[34,60] which are accessible by the void space within the structure. When crystals of IRMOF-3 were treated with dilute acetic anhydride at ambient temperature the amino groups were acylated (forming the expected amide) to generate a new material designated IRMOF-3-AM1. This transformation occurred not only in high yield but also with preservation of structural integrity and thermal stability of the MOF.

Upon completion of this initial study, several questions became apparent: (a) to what extent would IRMOF-3 be modified with larger reagents; (b) how would the physical properties (e.g., thermal stability, surface area, etc.) of IRMOF-3 change upon modification; and (c) how generally applicable is postsynthetic modification as a functionalization approach. Herein, we address these questions by expanding the modification of IRMOF-3 to transformations with 10 straight-chain alkyl anhydrides (with the general formula $O(CO(CH_2)_nCH_3)_2$, where $n = 1-18$). Modification products were characterized by $^1$H NMR and ESI-MS, and the extent of modification (i.e., % conversion) was quantified using $^1$H NMR. The integrity of modified IRMOF-3 samples was examined using TGA, PXRD, and single-crystal X-ray analysis. Brunauer−Emmett−Teller (BET) surface areas[61] were determined by measuring dinitrogen gas sorption to the modified MOFs. In all cases examined, IRMOF-3, while retaining its single crystallinity, thermal stability, and microporosity, was shown to be successfully modified. As a result, a series of new MOFs containing amide functionalities and alkyl chains of various lengths were readily generated; in the extreme case, a framework decorated with a significant amount of C-19 alkyl chains was obtained. The degree of modification appeared to be closely related to the length of anhydrides used. More importantly, the postsynthetic approach allowed for facile and reliable access to a family of closely related MOFs, which provided for a dependable evaluation and comparison of porosities in these compounds. It was found that both the degree of modification and the size of

(33) Rowsell, J. L. C.; Yaghi, O. M. *Angew. Chem., Int. Ed.* **2005**, *44*, 4670–4679.
(34) Eddaoudi, M.; Kim, J.; Rosi, N.; Vodak, D.; Wachter, J.; O'Keeffe, M.; Yaghi, O. M. *Science* **2002**, *295*, 469–472.
(35) Ma, S.; Sun, D.; Simmons, J. M.; Collier, C. D.; Yuan, D.; Zhou, H.-C. *J. Am. Chem. Soc.* **2008**, *130*, 1012–1016.
(36) Matsuda, R.; Kitaura, R.; Kitagawa, S.; Kubota, Y.; Belosludov, R. V.; Kobayashi, T. C.; Sakamoto, H.; Chiba, T.; Takata, M.; Kawazoe, Y.; Mita, Y. *Nature* **2005**, *436*, 238–241.
(37) Millward, A. R.; Yaghi, O. M. *J. Am. Chem. Soc.* **2005**, *127*, 17998–17999.
(38) Banerjee, R.; Phan, A.; Wang, B.; Knobler, C.; Furukawa, H.; O'Keeffe, M.; Yaghi, O. M. *Science* **2008**, *319*, 939–943.
(39) Custelcean, R.; Gorbunova, M. G. *J. Am. Chem. Soc.* **2005**, *127*, 16362–16363.
(40) Kawano, M.; Kawamichi, T.; Haneda, T.; Kojima, T.; Fujita, M. *J. Am. Chem. Soc.* **2007**, *129*, 15418–15419.
(41) Oh, M.; Carpenter, G. B.; Sweigart, D. A. *Acc. Chem. Res.* **2004**, *37*, 1–11.
(42) Kitagawa, S.; Noro, S.-i.; Nakamura, T. *Chem. Commun.* **2006**, 701–707.
(43) Halper, S. R.; Do, L.; Stork, J. R.; Cohen, S. M. *J. Am. Chem. Soc.* **2006**, *128*, 15255–15268.
(44) Kitaura, R.; Onoyama, G.; Sakamoto, H.; Matsuda, R.; Noro, S.-i.; Kitagawa, S. *Angew. Chem., Int. Ed.* **2004**, *43*, 2684–2687.
(45) Ma, S.; Zhou, H.-C. *J. Am. Chem. Soc.* **2006**, *128*, 11734–11735.
(46) Forster, P. M.; Eckert, J.; Heiken, B. D.; Parise, J. B.; Yoon, J. W.; Jhung, S. H.; Chang, J.-S.; Cheetham, A. K. *J. Am. Chem. Soc.* **2006**, *128*, 16846–16850.
(47) Dincă, M.; Dailly, A.; Liu, Y.; Brown, C. M.; Neumann, D. A.; Long, J. R. *J. Am. Chem. Soc.* **2006**, *128*, 16876–16883.
(48) Inagaki, S.; Guan, S.; Ohsuna, T.; Terasaki, O. *Nature* **2002**, *416*, 304–307.
(49) Yang, Q.; Kapoor, M. P.; Inagaki, S. *J. Am. Chem. Soc.* **2002**, *124*, 9694–9695.
(50) Hirsch, A. *Angew. Chem., Int. Ed.* **2002**, *41*, 1853–1859.
(51) Kiang, Y.-H.; Gardner, G. B.; Lee, S.; Xu, Z.; Lobkovsky, E. B. *J. Am. Chem. Soc.* **1999**, *121*, 8204–8215.
(52) Xu, Z.; Lee, S.; Kiang, Y.-H.; Mallik, A. B.; Tsomaia, N.; Mueller, K. T. *Adv. Mater.* **2001**, *13*, 637–641.
(53) Wang, X.-S.; Ma, S.; Sun, D.; Parkin, S.; Zhou, H.-C. *J. Am. Chem. Soc.* **2006**, *128*, 16474–16475.
(54) Mulfort, K. L.; Hupp, J. T. *J. Am. Chem. Soc.* **2007**, *129*, 9604–9605.
(55) Haneda, T.; Kawano, M.; Kawamichi, T.; Fujita, M. *J. Am. Chem. Soc.* **2008**, *130*, 1578–1579.
(56) Kaye, S. S.; Long, J. R. *J. Am. Chem. Soc.* **2008**, *130*, 806–807.
(57) Ingleson, M. J.; Barrio, J. P.; Bacsa, J.; Dickinson, C.; Park, H.; Rosseinsky, M. J. *Chem. Commun.* **2008**, 1287–1289.
(58) Costa, J. S.; Gamez, P.; Black, C. A.; Roubeau, O.; Teat, S. J.; Reedijk, J. *Eur. J. Inorg. Chem.* **2008**, 1551–1554.
(59) Wang, Z.; Cohen, S. M. *J. Am. Chem. Soc.* **2007**, *129*, 12368–12369.
(60) Rowsell, J. L. C.; Yaghi, O. M. *J. Am. Chem. Soc.* **2006**, *128*, 1304–1315.
(61) Walton, K. S.; Snurr, R. Q. *J. Am. Chem. Soc.* **2007**, *129*, 8552–8556.

*Scheme 1*[a]

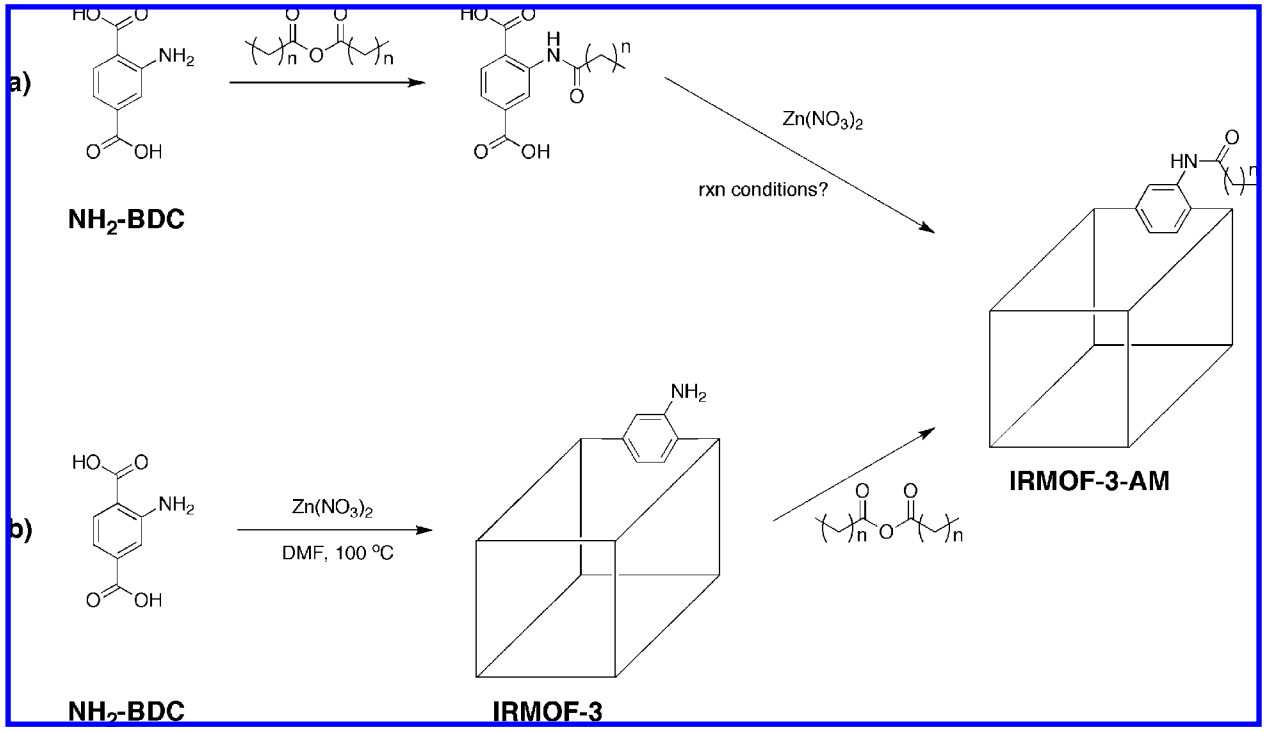


[a] (a) The conventional approach to MOF functionalization using a modified precursor, and (b) the postsynthetic modification approach to the same MOF.

substituents affect the outcomes. Thus, the "late-stage" functionalization approach[62] we describe herein provides an important alternative to traditional MOF synthesis, achieves better atom economy,[63] and affords an efficient route to the systematic functionalization of MOFs (Scheme 1).

## Experimental Methods

**Preparation of IRMOF-3.** Starting reagents and solvents were purchased and used without further purification from commercial suppliers (Sigma-Aldrich, Alfa Aesar, EMD, TCI, Cambridge Isotope Laboratories, Inc., and others). IRMOF-3 was synthesized and activated according to a modified procedure from literature.[60] $Zn(NO_3)_2 \cdot 4H_2O$ (6.00 g, 22.9 mmol) and 2-aminobenzenedicarboxylic acid (1.50 g, 8.30 mmol) were dissolved in 200 mL of DMF. The solution was divided into 10 mL portions and transferred to 20 scintillation vials (20 mL capacity). The vials were placed in a sand bath, and the bath was transferred to a programmable oven and heated at a rate of 2.5 °C/min from 35 to 100 °C. The temperature was held for 18 h, and then the oven was cooled at a rate of 2.5 °C/min to a final temperature of 35 °C. This procedure generated amber block crystals of IRMOF-3. The mother liquor from each vial was decanted, and the crystals were washed with dry DMF (3 × 12 mL) (dried over molecular sieves) followed by one rinse with 12 mL of $CHCl_3$. The crystals were then soaked in 12 mL of $CHCl_3$ for 3 days with fresh $CHCl_3$ added every 24 h. After 3 days of soaking the crystals were stored in the last $CHCl_3$ solution until needed. The average yield of dried IRMOF-3 per vial was determined to be approximately 55−60 mg (∼50%).

**Method 1. Postsynthetic Modification Using Dry IRMOF-3.** For each alkyl anhydride examined, five 4 mL dram vials were prepared in order to monitor the reactivity of IRMOF-3 over a period of five days. The $CHCl_3$ storage solution of IRMOF-3 was decanted, and the crystals were dried at 75 °C under vacuum for 12 h. Dried IRMOF-3 (27 mg, ca. 0.10 mmol equiv of $-NH_2$) was suspended in 1.0 mL of $CDCl_3$ in a 4 mL dram vial. Alkyl anhydride (2 equiv, 0.20 mmol for $n = 1$ to 15; 0.8 equiv, 0.08 mmol for $n = 18$) was added to the $CDCl_3$ solution, and the mixture was left to react at room temperature. The $CDCl_3$ solution was removed from one vial every 24 h and set aside for $^1$H NMR analysis of the soluble reaction byproducts (vide infra). After removal of the $CDCl_3$ solution, the modified IRMOF-3 crystals were washed with $CH_2Cl_2$ (3 × 2 mL) and left to soak in 2 mL of $CH_2Cl_2$ for 3 days, with fresh $CH_2Cl_2$ added every 24 h. After 3 days, the $CH_2Cl_2$ solution was decanted and the modified IRMOF-3 crystals were dried at 90 °C under vacuum for 8 h. Samples prepared in this fashion were analyzed using $^1$H NMR, ESI-MS, TGA, and PXRD.

**Method 2. Postsynthetic Modification Using Wet IRMOF-3.** Approximately 55−60 mg of IRMOF-3 (ca. 0.2 mmol equiv of $-NH_2$) were placed in a vial with 2 equiv (0.4 mmol for $n = 1$ to 15) or 0.8 equiv (0.16 mmol for $n = 18$) of alkyl anhydride dissolved in either 8 mL ($n = 1, 2, 3$) or 4 mL ($n = 4, 5, 6, 8, 12, 15, 18$) of $CHCl_3$. The different dilutions (i.e., anhydride concentrations) were used in order to best preserve the single crystallinity of the samples. After allowing the sample ($n = 1$ to 12) to stand at room temperature for 24 h, the solution was decanted and the crystals were washed with $CHCl_3$ (3 × 5 mL). A fresh solution of the anhydride was added to the vial, and the crystals were left to stand for an additional 24 h. The aforementioned procedure was repeated (washing followed by treatment with anhydride), with the only difference that some anhydrides ($n = 1, 2, 3$) were replenished at half the original concentration (1 equiv, 0.2 mmol in 8 mL of $CHCl_3$ for $n = 1, 2, 3$), giving a total reaction time of 3 days. Other samples ($n = 15, 18$) were treated for 3 days without replacing the anhydride solution. The $CHCl_3$ solution was decanted, and the crystals were washed with $CHCl_3$ (3 × 5 mL) before soaking in 5 mL of pure $CHCl_3$ for 3 days, with fresh $CHCl_3$ added every 24 h. After 3 days of soaking the crystals were stored in the last $CHCl_3$ solution until needed. Samples prepared in this fashion were analyzed using $^1$H NMR, ESI-MS, gas sorption, and single-crystal X-ray diffraction (when applicable).

**Digestion and Analysis by $^1$H NMR.** $^1$H NMR spectra were recorded on Varian FT-NMR spectrometers (400 and 500 MHz).

(62) Chen, M. S.; White, M. C. *Science* **2007**, *318*, 783–787.
(63) Trost, B. M. *Angew. Chem., Int. Ed. Engl.* **1995**, *34*, 259–281.

Approximately 5 mg of IRMOF-3 modified using either Method 1 or Method 2 were digested by sonication in 500 $\mu$L of $d^6$-DMSO and 100 $\mu$L of dilute DCl (23 $\mu$L of 35% DCl in $D_2O$ diluted with 1 mL of $d^6$-DMSO). Upon complete dissolution of the crystals, this solution was used for $^1$H NMR analysis.

**Digestion and Analysis by MS.** Electrospray ionization mass spectrometry (ESI-MS) was performed using a ThermoFinnigan LCQ-DECA mass spectrometer, and the data were analyzed using the Xcalibur software suite. Samples for analysis by ESI-MS were prepared by digesting the single crystal from X-ray analysis (vide infra) in 200−300 $\mu$L of $H_2O$ or MeOH and were analyzed in negative ion mode.

**Thermal Analysis.** Approximately 10−12 mg of IRMOF-3 modified using Method 1 were used for TGA measurements. Samples were analyzed under a stream of dinitrogen using a TA Instrument Q600 SDT running from 25 to 600 °C with a scan rate of 5 °C/min.

**PXRD Analysis.** Approximately 15 mg of IRMOF-3 modified using Method 1 were soaked in 2 mL of fresh $CHCl_3$ for 2 days prior to analysis. Powder X-ray diffraction (PXRD) data were collected at ambient temperature on a Rigaku Miniflex II diffractometer at 30 kV, 15 mA for Cu K$\alpha$ ($\lambda$ = 1.5418 Å), with a scan speed of 5°/min and a step size of 0.05° in 2$\theta$.

**BET Surface Analysis.** Approximately 60−75 mg of modified IRMOF-3 using Method 2 were evacuated under vacuum overnight. The modified IRMOF-3 was transferred to a preweighed sample tube and degassed at 30 °C for approximately 24 h on an ASAP 2020 or until the outgas rate was <5 $\mu$mHg. The sample tube was reweighed to obtain a consistent mass for the degassed modified IRMOF-3. BET surface area ($m^2$/g) measurements were collected at 77 K by dinitrogen on an ASAP 2020.

**Single-Crystal X-ray Diffraction.** Single crystals of modified IRMOF-3 soaking in $CHCl_3$ were mounted on nylon loops with Paratone oil and placed under a nitrogen cold stream (200 K). Data were collected on Bruker Apex diffractometers using Mo K$\alpha$ radiation ($\lambda$ = 0.710 73 Å) controlled using the APEX 2.0 software package. Cell determinations were performed on all modified IRMOF-3, and full data sets were collected on four modifications of IRMOF-3 (-AM4, -AM6, -AM13, and -AM19). A semiempirical method utilizing equivalents was employed to correct for absorption.[64] All data collections were solved and refined using the SHELXTL suite. All non-hydrogen atoms were refined anisotropically. IRMOF-3-AM4, -AM6, -AM13, and -AM19 were treated with the "squeeze" protocol in PLATON[65] to account for electron density associated with the disordered alkyl substituent $-CO(CH_2)_nCH_3$ and for partially occupied or disordered solvent (e.g., $CHCl_3$) within the porous framework. The empirical formulas were adjusted to accommodate the appropriate ratio of unmodified $NH_2$–BDC to modified alkyl amide BDC ligand; solvent was not included, but was noted in the CIF.

## Results

**Modification of IRMOF-3 with Alkyl Anhydrides.** The reactivity of 10 alkyl anhydrides with IRMOF-3 was examined using two different procedures: "Method 1" utilizes samples of IRMOF-3 that were extensively washed and then dried under vacuum at 75 °C for 12 h, while "Method 2" uses IRMOF-3 samples that were washed, but were not dried prior to postsynthetic modification. These two methods were used to examine several features of the modified IRMOFs and also to compare the effects of sample preparation on the efficiency of the modification reaction. The more pristine samples prepared by Method 2 were specifically used for obtaining single-crystal X-ray diffraction data and BET surface area measurements (vide infra).

As described in an earlier report,[59] acetic acid is generated as a reaction byproduct upon modification of IRMOF-3 with acetic anhydride. Therefore, to monitor the progress of postsynthetic modification reactions, the $CDCl_3$ supernatant from IRMOF-3 samples (prepared via Method 1) was examined by $^1$H NMR to monitor the conversion of the reactive anhydrides to corresponding carboxylic acid byproducts. The distinct upfield shift of the $\alpha$-$CH_2$ for each of the carboxylic acids generated from the reaction with the various anhydrides allows for an indirect determination of the progress of the reaction with IRMOF-3 without destruction of the MOF sample. $^1$H NMR spectra of the reaction with each alkyl anhydride were complied to compare the ratio of anhydride to acid byproduct over time (Supporting Information). A representative set of spectra is shown in Figure 1. Before the start of the reaction, only the peaks corresponding to the unreacted hexanoic anhydride ($n$ = 4) are present. After 24 h, a triplet peak, indicative of the acid byproduct, appears in the spectra. The triplet peak of the acid byproduct continues to increase indicating that IRMOF-3 is reacting with the anhydride to produce IRMOF-3-AM5. By day 5, IRMOF-3-AM5 was approximately ~94% modified based on $^1$H NMR of the digested sample (vide infra). A qualitative correlation between acid byproduct formation and the percent conversion of IRMOF-3 was observed. Smaller chain anhydrides, which gave high conversions, generated larger amounts of acid byproduct when compared with longer chain anhydrides, which produced smaller amounts of acid byproduct and showed expectedly lower conversions.

After monitoring the reaction supernatant for 5 days, modified IRMOF-3 samples were digested in a $d^6$-DMSO/DCl solution and analyzed by $^1$H NMR to quantitatively measure the percent conversion of $NH_2$−BDC to the respective amide-modified dicarboxylate (Table 1). Percent conversion was calculated by relative integration of the aromatic single resonance (Figure 2), which corresponds to the phenyl proton adjacent to the amine/amide group (C-3 position) on the BDC ligand. Integration of the modified singlet over the summation of both the modified IRMOF-3 and unmodified IRMOF-3 aromatic singlets was used to determine the conversion values. IRMOF-3 underwent reactions with all anhydrides tested, with conversions ranging from 97% (-AM2) to 11% (-AM19). Increasing chain length resulted in a drop in percent conversion, particularly beyond $n$ > 6. The most drastic decreases were seen between IRMOF-3-AM7 and IRMOF-3-AM9, IRMOF-3-AM9 and IRMOF-3-AM13, and IRMOF-3-AM16 and IRMOF-3-AM19 where the addition of a few methylene groups resulted in 20−30% drops in modification.

The effect of sample preparation on percent conversion was determined by performing a set of parallel experiments with single crystals of IRMOF-3 prepared by Method 2. A very high quality of crystallinity could be preserved by not heating or drying the crystals, as evidenced visually and by single-crystal X-ray diffraction experiments (vide infra). IRMOF-3 samples prepared by Method 2 were treated with anhydrides under slightly modified reaction conditions, including daily exchanges of fresh anhydride for $n$ = 1 to 12. Optimization of the reaction conditions revealed that after 3 days, with concentrations of anhydride varying from 0.05 to 0.1 M, a combination of significant modification and good crystallinity could be achieved. Under these conditions (Method 2), IRMOF-3 samples showed

(64) Sheldrick, G. M. *SADABS (The semiempirical method used is based on a method of Blessing, R. H. Acta Crystallogr. 1995, A51, 33)*, version 2.10; Bruker AXS, Inc.: Madison, WI, 2004.
(65) Spek, A. L. *J. Appl. Crystallogr.* **2003**, *36*, 7–13.

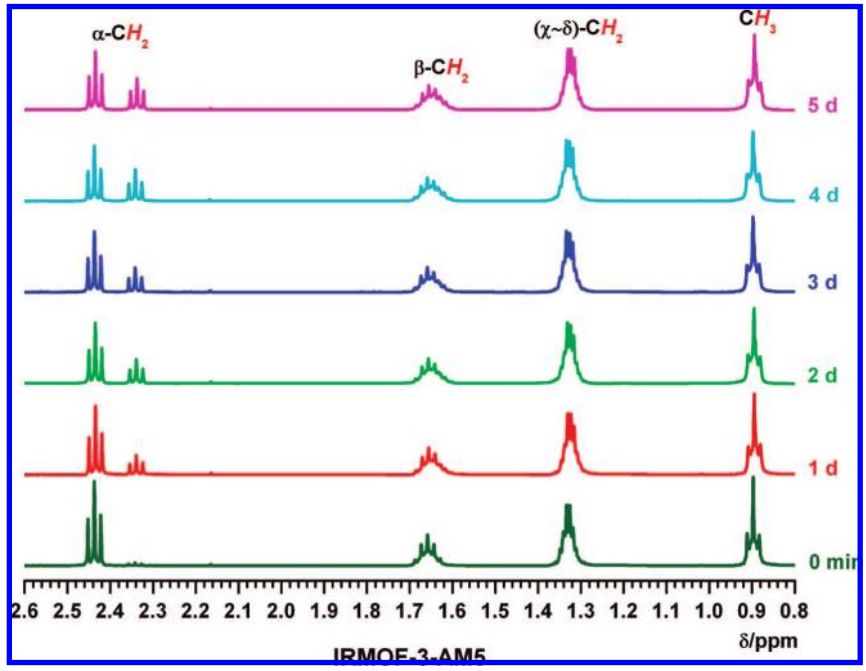


***Figure 1.*** $^1$H NMR spectra of the reaction mixture of IRMOF-3 modified with hexanoic anhydride ($n = 4$) collected between 0 and 5 days. Each spectrum is normalized to the α-$CH_2$ resonance of hexanoic anhydride. Reaction conditions: rt, $CDCl_3$ (1.00 mL), IRMOF-3 crystals (Method 1, 0.10 mmol equiv of $-NH_2$), and anhydride (0.20 mmol).

***Table 1.*** Percent Conversions of IRMOF-3 with Different Anhydrides as Determined by $^1$H NMR[a]

| IRMOF-3 | -AM2 | -AM3 | -AM4 | -AM5 | -AM6 | -AM7 | -AM9 | -AM13 | -AM16 | -AM19 |
|---|---|---|---|---|---|---|---|---|---|---|
| $n =$ | 1 | 2 | 3 | 4 | 5 | 6 | 8 | 12 | 15 | 18 |
| Method 1[c] | 97 ± 3% | 98 ± 3% | 97 ± 3% | 94 ± 5% | 90 ± 5% | 81 ± 5% | 51 ± 5% | 31 ± 5% | 30 ± 2% | 11 ± 1%[b] |
| Method 2[d] | ~99% | ~99% | 98 ± 3% | 96 ± 3% | 90 ± 3% | 80 ± 5% | 46 ± 7% | 32 ± 5% | 20 ± 1% | 7 ± 1%[b] |

[a] Values listed are an average (with standard deviations) of at least three independent experiments for Method 1 and four independent experiments for Method 2. [b] 0.8 equiv of anhydride was used (instead of 2 equiv) due to low solubility of the reagent. [c] Total reaction time of 5 days. [d] Total reaction time of 3 days.

conversions from 7% ($n = 18$) to essentially quantitative (~99%, $n = 1$) based on $^1$H NMR analysis of the digested samples (Table 1).

**Thermal and Structural Stability of Modified IRMOF-3.** Visually, all modified IRMOF samples, prepared by either method, showed no signs of degradation and maintained their block-like appearance after complete treatment (3 to 5 days). In order to confirm the stability and structural integrity of the modified IRMOF-3, samples of IRMOF-3-AM-2 to IRMOF-3-AM19 (prepared by Method 1 after 5 days of treatment with anhydride) were examined by TGA and PXRD methods. Samples analyzed by TGA were dried under vacuum to remove any residual solvent. All of the modified IRMOF samples showed comparable thermal stability to IRMOF-3 with decomposition temperatures of ~430 °C (Figure 3). Likewise, phase purity and bulk crystallinity were verified by PXRD measurements. All modified IRMOF-3 samples (prepared by Method 1) showed preservation of crystallinity, and all $2\theta$ peaks were consistent with as-synthesized IRMOF-3 (Figure 4, Figure S1). The uniformity of all $2\theta$ peaks for each modified IRMOF-3 sample shows that modification has no effect on the overall structural integrity of the framework. More importantly, all modified IRMOF-3 samples show no phase or structural differences based on the reactivity of anhydride used or the degree of modification.

**Single-Crystal X-ray Analysis of Modified IRMOF-3.** To demonstrate the high structural integrity of IRMOF-3 under postsynthetic modification conditions, single-crystal X-ray data were collected for all modified IRMOF-3 samples (prepared via Method 2). Only unit cell determinations were performed for most samples (Table 2), but complete data sets were obtained for IRMOF-3-AM4, -AM6, -AM13, and -AM19 (Table 3). As evidenced by these analyses, all of the samples maintained single crystallinity under the reaction conditions (Figures S11−S20). To unambiguously confirm that the samples had undergone acylation, each single crystal was removed from the diffractometer after data collection, digested in $H_2O$ or MeOH, and analyzed by negative ion mode ESI-MS; in every case the base peak observed was the expected $[M - H]^-$ ion of the modified BDC ligand (Figures S21−S30).

All modified IRMOF-3 cell determinations showed no significant change in the cell parameters by comparison with IRMOF-3. IRMOF-3 has a cubic structure (space group $Fm\bar{3}m$) with $a = b = c = 25.7465(14)$ Å, $\alpha = \beta = \gamma = 90°$, and a unit cell volume of 17066.0(16) Å$^3$.[34] As expected for a single-crystal-to-single-crystal transformation, all of the modified IRMOF-3 samples possessed the same crystal system and cell setting (cubic, $F$ centered) with $a = b = c \approx 25$ Å, $\alpha = \beta = \gamma = 90°$, and unit cell volumes of ~17000 Å$^3$ (Tables 2 and 3). Unambiguous proof of the single-crystal-to-single-crystal transformation for these MOFs was obtained with four complete data collections for IRMOF-3 modified with short alkyl anhydrides ($n = 3, 5$) and long alkyl anhydrides ($n = 12, 18$). These complete data sets (Table 3) gave satisfactory solutions

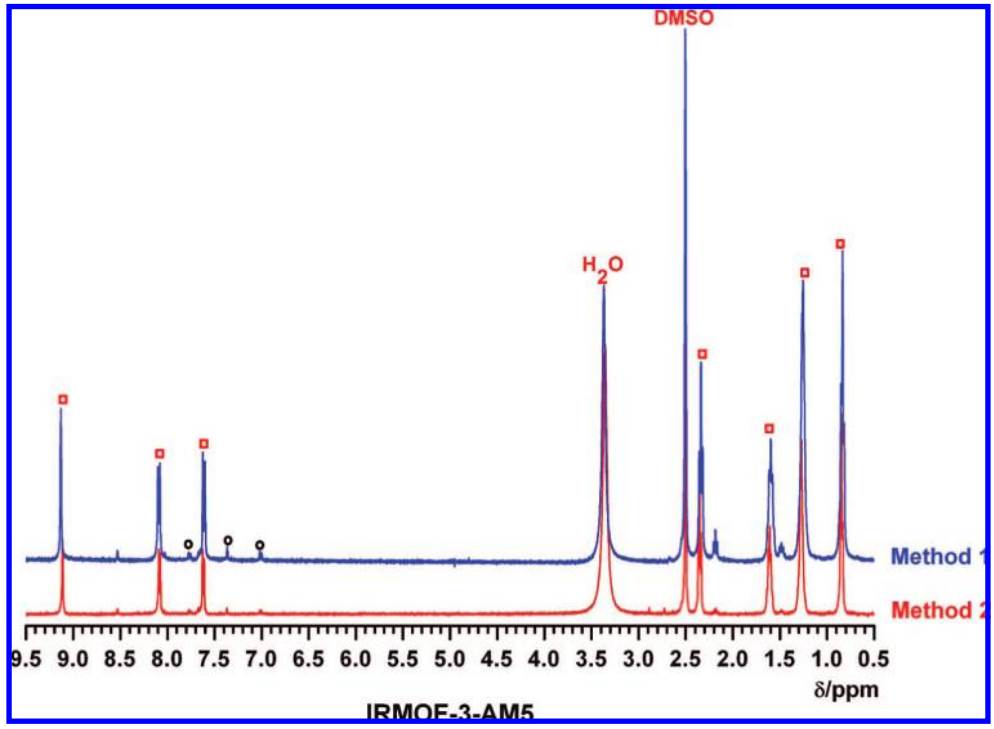


***Figure 2.*** $^{1}$H NMR spectra of digested IRMOF-3 modified with hexanoic anhydride ($n = 4$) via Method 1 (5 days) and Method 2 (3 days). IRMOF-3-AM5 samples (5 mg) were dried at 90 °C for 8 h and digested in 500 $\mu$L of $d^6$-DMSO and 100 $\mu$L of DCl solution (23 $\mu$L of 35% DCl in $D_2O$ and 1 mL of $d^6$-DMSO) with sonication. Labeled peaks represent $NH_2-$BDC (black circles) and the acylated reaction product (red squares).

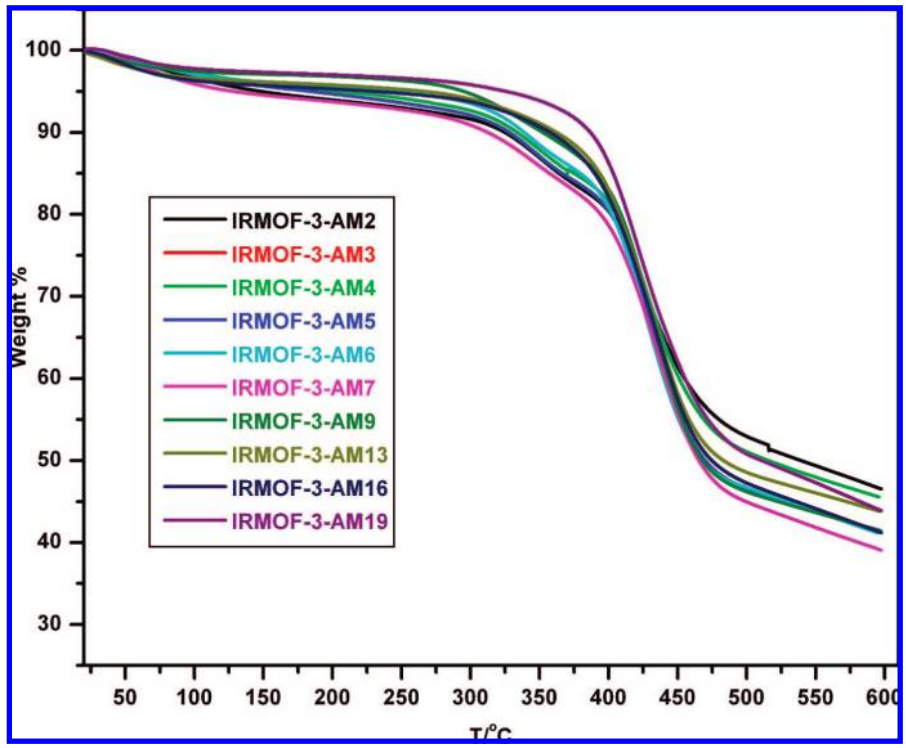


***Figure 3.*** Thermogravimetric analysis (TGA) of modified IRMOF-3 samples. All samples were previously dried at 90 °C under vacuum for 8 h. Modified IRMOF-3 (10−12 mg) was heated at a scan rate of 5 °C/min from 25 to 600 °C.

that showed the expected MOF lattice comprised of BDC ligands and the $Zn_4O$ SBUs.

Although high-quality single crystals were used for these data collections, none of the modified IRMOF-3 samples showed substantial electron density for the alkyl-amide substituent. The substituent cannot be experimentally located for these modified IRMOF-3 samples due to disorder over the four positions on the BDC ligand.[34,58] Because the substituent could not be identified in the full data collections for IRMOF-3-AM4, -AM6, -AM13, and -AM19, each single crystal used for X-ray analysis was digested for ESI-MS analysis to confirm the presence of the modified BDC ligand. All single crystals showed the

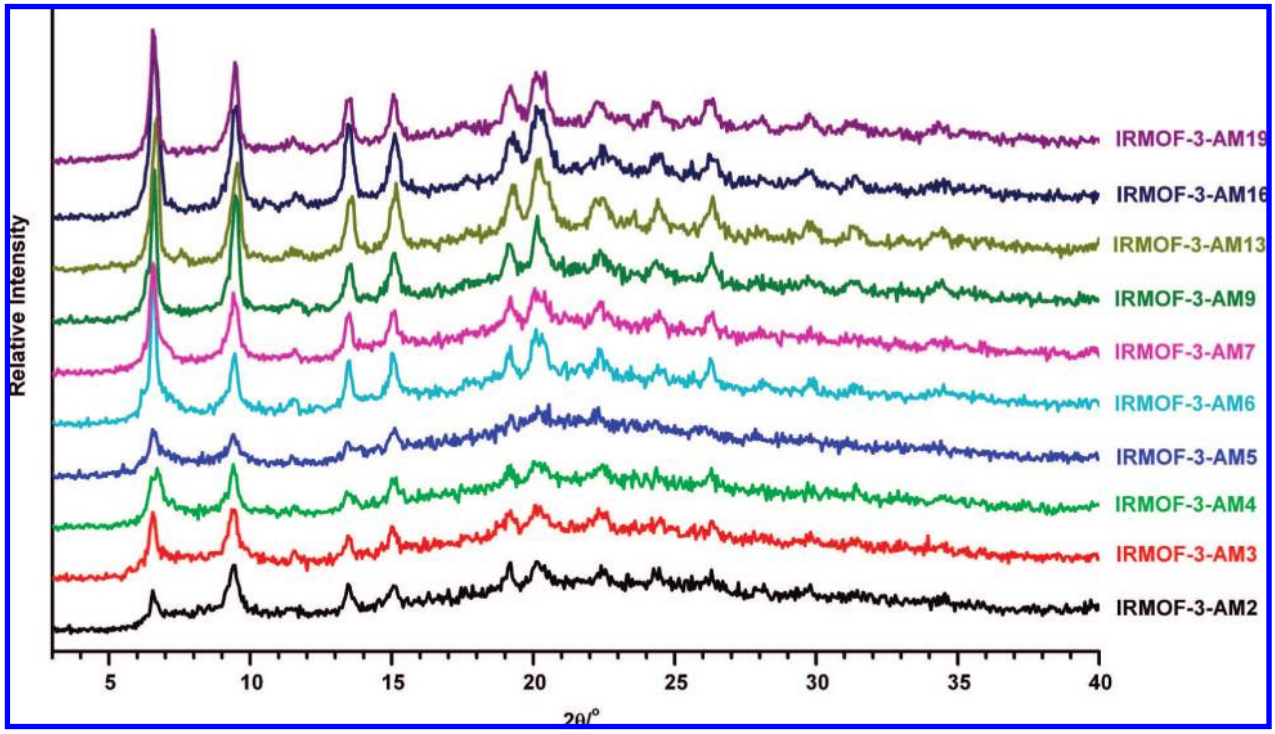


***Figure 4.*** Powder X-ray diffraction (PXRD) patterns of modified IRMOF-3 samples (Method 1). Modified IRMOF-3 samples were soaked and exchanged with fresh $CHCl_3$ for 2 days. After decanting off the solvent, the samples were left drying in air for one hour prior to PXRD analysis.

***Table 2.*** Unit Cell Determinations and Mass Spectrometry Data for Modified IRMOF-3 Single Crystals

| IRMOF-3 | -AM2 | -AM3 | -AM5 | -AM7 | -AM9 | -AM16 |
|---|---|---|---|---|---|---|
| morphology | block | block | block | block | block | block |
| size (mm) | 0.33 | 0.40 | 0.33 | 0.50 | 0.51 | 0.30 |
| | 0.31 | 0.33 | 0.31 | 0.35 | 0.27 | 0.30 |
| | 0.31 | 0.28 | 0.25 | 0.34 | 0.20 | 0.25 |
| cell setting | cubic *F* | cubic *F* | cubic *F* | cubic *F* | cubic *F* | cubic *F* |
| $a = b = c$ | 25.53 | 25.74 | 25.65 | 25.73 | 25.68 | 25.97 |
| $\alpha = \beta = \gamma$ | 90° | 90° | 90° | 90° | 90° | 90° |
| volume (Å$^3$) | 16 639 | 17 054 | 16 876 | 17 036 | 16 943 | 17 519 |
| ESI-MS(−) $[M - H]^-$ | 236 | 250 | 278 | 306 | 334 | 432 |

expected amide-modified BDC ligand and confirmed the composition of the crystals.

**Gas Sorption of Modified IRMOF-3.** BET surface area measurements were collected in order to evaluate the microporosity of the modified IRMOF-3 samples. For these studies, two BET measurements were averaged for each modified IRMOF-3 to determine whether a correlation between porosity and the alkyl chain length could be discerned. All crystalline modified IRMOF-3 samples were run at 77 K with dinitrogen, and all were found to retain porosity despite differing degrees of modification. From IRMOF-3-AM2 to IRMOF-3-AM6, the BET surface area gradually decreases, likely due to a combination of high conversion (>90%) and increasing alkyl chain length filling the pores. The BET surface area measurements were found to range from 1641 to 1165 $m^2/g$ for IRMOF-3-AM2 to -AM6. For IRMOF-3-AM7, where the percent conversion begins to drop below 90%, the measured BET surface area rises to 1185 $m^2/g$. Surprisingly, for the rest of the modified IRMOFs, a reverse trend is observed of increasing surface area with increasing alkyl chain length. The BET surface area measurements were found to rise from 1185 to 2164 $m^2/g$ from IRMOF-3-AM7 to -AM19.

## Discussion

**Solid-State Reactivity of IRMOF-3 with Alkyl Anhydrides.** The heterogeneous nature of the postsynthetic modification of MOFs, which involves solid-phase, crystalline MOFs immersed in liquid solutions containing organic reagents, imparts some unique features that distinguish the process from traditional chemical reactions performed in a homogeneous medium. For example, one would expect that the steric effects might play a more critical role in modulating the kinetics of postsynthetic modification reactions because the diffusion of reagents and, in some cases, the elution of reaction byproducts will inevitably be influenced by the size of pores within the MOF lattice. Indeed, we have observed a reasonable trend of reactivity toward IRMOF-3 for 10 alkyl anhydrides. Conversion of IRMOF-3 to the modified MOFs, as prepared by Method 1, clearly suggests that under similar conditions (i.e., nearly identical reactant concentrations and reaction times) the degree of modification correlates to the size of the anhydride (Figure 5). For shorter anhydrides ($n \leq 5$), IRMOF-3 conversion is essentially quantitative after 5 days, implying negligible steric hindrance between these anhydrides and the MOF lattice; for longer anhydrides ($n > 5$), size effects become significant, with IRMOF-3 being only partially modified, decreasing as the size of the anhydride increases. Samples prepared by Method 2 reveal a very similar tendency, albeit with slightly lower conversions with longer anhydrides, likely due to the milder conditions employed by Method 2 (Table 1). This chain-length dependent reactivity of alkyl anhydrides toward IRMOF-3 can be accounted for by considering, in addition to the diffusion problems, the difficulty of accommodating longer substituents by the MOF. However, it should also be noted that other factors, such as the intrinsically different reactivity of these anhydrides,

***Table 3.*** Structure Determination Parameters and Mass Spectrometry Data for Modified IRMOF-3 Single Crystals

| IRMOF-3 | -AM4 | -AM6 | -AM13 | -AM19 |
|---|---|---|---|---|
| formula[a] | $C_{39}H_{39}N_3O_{16}Zn_4$ | $C_{42.90}H_{47.40}N_3O_{15.70}Zn_4$ | $C_{40.80}H_{46.20}N_3O_{14.20}Zn_4$ | $C_{27.90}H_{22.41}N_3O_{13.21}Zn_4$ |
| morphology | block | block | block | block |
| color | amber | amber | amber | amber |
| size (mm) | 0.30 | 0.34 | 0.43 | 0.41 |
| | 0.20 | 0.32 | 0.39 | 0.32 |
| | 0.20 | 0.27 | 0.29 | 0.24 |
| crystal system | cubic | cubic | cubic | cubic |
| space group | *Fm*-3*m* | *Fm*-3*m* | *Fm*-3*m* | *Fm*-3*m* |
| $a = b = c$ | 25.7386(6) | 25.7228(6) | 25.7691(17) | 25.7786(7) |
| $\alpha = \beta = \gamma$ | 90° | 90° | 90° | 90° |
| volume (Å$^3$) | 17051.2(7) | 17019.8(7) | 17112(2) | 17130.8(8) |
| *T*, K | 200(2) | 200(2) | 200(2) | 200(2) |
| reflns measured | 6694 | 6551 | 3216 | 9407 |
| data/restraints/parameters | 935/0/28 | 845/0/28 | 701/0/30 | 832/0/28 |
| independent reflns | 935 | 845 | 701 | 832 |
| [*R*(int)] | [*R*(int) = 0.0361] | [*R*(int) = 0.0193] | [*R*(int) = 0.0178] | [*R*(int) = 0.0289] |
| final *R* indices | *R*1 = 0.0304, | *R*1 = 0.0349, | *R*1 = 0.0368, | *R*1 = 0.0351, |
| $[I > 2\sigma(I)]$[a] | *wR*2 = 0.0814 | *wR*2 = 0.1047 | *wR*2 = 0.1140 | *wR*2 = 0.1035 |
| *R* indices (all data, | *R*1 = 0.0387, | *R*1 = 0.0395, | *R*1 = 0.0407, | *R*1 = 0.0405, |
| $F^2$ refinement)[a] | *wR*2 = 0.0849 | *wR*2 = 0.1081 | *wR*2 = 0.1207 | *wR*2 = 0.1078 |
| GOF on $F^2$ | 0.918 | 1.082 | 1.165 | 1.071 |
| largest diff. peak and hole, e/A$^3$ | 0.357 and −0.207 | 0.297 and −0.278 | 0.474 and −0.287 | 0.522 and −0.267 |
| ESI-MS(−) $[M - H]^-$ | 264 | 292 | 390 | 474 |

[a] The empirical formulas reflect the appropriate ratio of unmodified amino-BDC to modified alkyl amide BDC ligand.

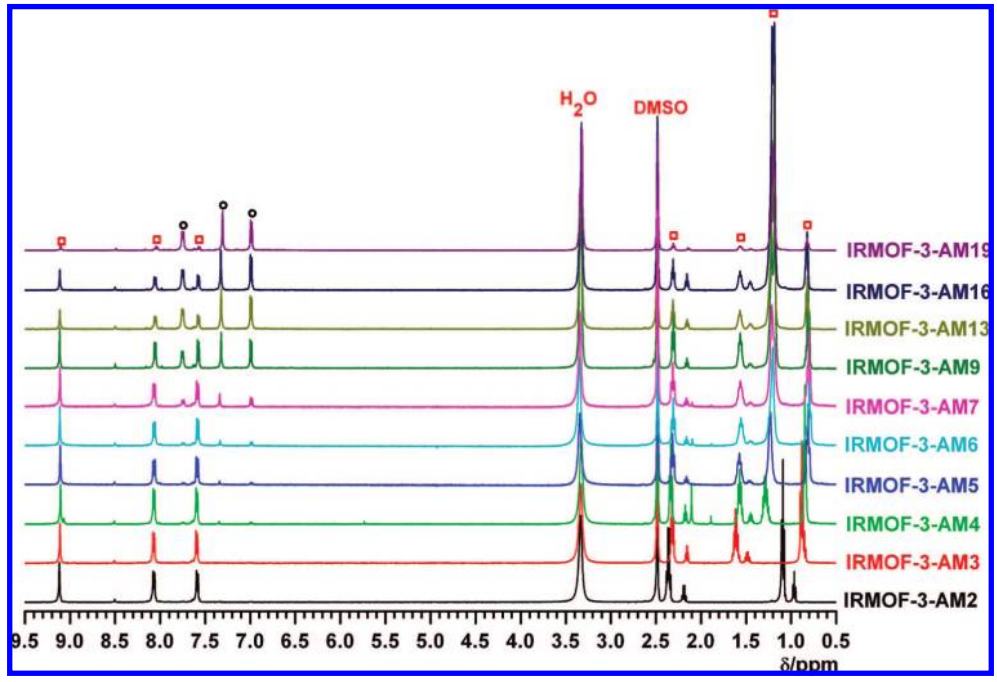


***Figure 5.*** $^1$H NMR spectra of digested IRMOF-3 samples (Method 1). Each spectrum was normalized either to the singlet at 9.1 ppm ($n \leq 8$) or to the singlet at 7.3 ppm ($n > 8$). Reaction conditions: rt, 5 d, $CDCl_3$ (1.00 mL), IRMOF-3 crystals (0.10 mmol equiv of $-NH_2$), and anhydride (0.20 mmol for $n = 1$ to 15, 0.08 mmol for $n = 18$). Each sample (5 mg) was dried at 90 °C for 8 h and digested in 500 $\mu$L of $d^6$-DMSO and 100 $\mu$L of DCl solution (23 $\mu$L of 35% DCl in $D_2O$ and 1 mL of $d^6$-DMSO) with sonication.

might also contribute to the general trend of modification kinetics. Also, we expect that the reaction conditions may be further adjusted to increase the percent conversion of IRMOF-3 with some of the longer chain anhydrides.

It should also be briefly mentioned that, in the $^1$H NMR spectra of the digested modified samples, small peaks of signals that are associated with the corresponding free acids are also noted in the upfield region (Figures 2 and 5). We previously speculated that the acid was due to hydrolysis of the modified ligand upon digestion.[59] However, accumulating evidence strongly suggests that the observed acid is due to trapping of byproducts during modification within the MOF lattice.

Other important characteristics of the heterogeneous modification of MOFs include a high degree of control over the reaction course and the ease of product isolation. As demonstrated by Methods 1 and 2, both reactant concentrations and reaction times are easily changed, enabling effective control over the consistency of materials preparation and convenient access to high-quality products. More importantly, no extra measures are required for the isolation of modified IRMOF-3 samples,

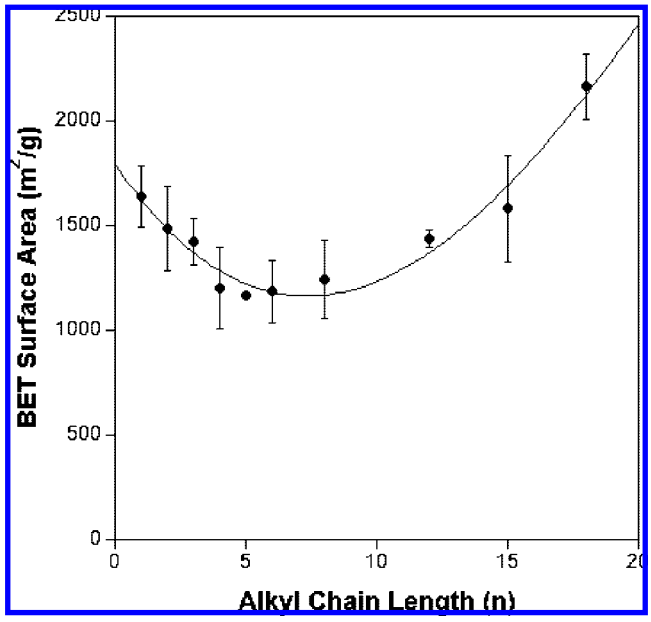


***Figure 6.*** Plot of BET surface area of modified IRMOF-3 as a function of alkyl chain length.

as separating solid products from liquid media is straightforward. These features draw a clear contrast to the homogeneous reactions where isolation and purification of products are often tedious and sometimes even quite challenging. The postsynthetic modification approach is thus well suited for MOF functionalization from a practical perspective.

The fact that IRMOF-3 samples have been only partially modified by some anhydrides (e.g., $n > 5$) also raises an intriguing question that concerns the spatial distribution of the newly introduced substituents within the MOF lattice and hence the reconfiguration of the pore structures. In principle, there exist at least two possible models for the distribution of the modifications within the MOF. In one case, the limited number of amide groups is concentrated on the outer layers of the lattice (including the surface) with the inner core of the MOF essentially unchanged. In the second case, the modifications may simply be evenly distributed throughout the entire framework. Further study is necessary in order to distinguish between these two possibilities, although a recent study by Fujita et al.[55] suggests that the postsynthetic modification of an MOF appears to follow the first model. We speculate that the outcomes are largely dependent upon both the rate of reagent diffusion and reactivity of the reagents. If the diffusion is slower than the reaction rate, the first model is more likely to follow; if the diffusion is faster than the reaction rate, the second model might occur.

**Systematic Functionalization of IRMOF-3.** Prior to this present report, a small number of studies reported the postsynthetic modification protocol and took advantage of some well-established chemical reactions to functionalize MOFs.[20,55,59] However, the generality of this "late-stage" functionalization strategy has remained unclear. By following the same postsynthetic principles and focusing upon a simple amide coupling reaction, we have generated a large number of new functionalized MOFs, namely, IRMOF-3-AM2 to IRMOF-3-AM19, and have therefore not only expanded the scope of this approach but also highlighted its efficiency as well as synthetic utility. Considering the high quality (i.e., single crystallinity, high porosity, and thermal stability) and modulated properties (i.e., increasing hydrophobicity) of these new materials, it appears clear that the atom economy achieved by the postsynthetic modification approach may be superior to traditional MOF synthetic methods (Scheme 1) for systematically generating a series of MOFs as described here.

More importantly, our modification method has led to some novel MOF structures that might be far more challenging to obtain from the traditional synthetic route. Comparison of percent conversions (Table 1) indicates that increasing reactant concentration and reaction duration (Method 1 vs Method 2) does not dramatically augment the degree of modification for longer anhydrides ($n \geq 8$), suggesting a fully substituted version of these MOFs might not be favored or feasible at all. In addition, the highly hydrophobic nature of long alkyl chains might further complicate solvothermal synthesis due to polarity and solubility of the ligand precursor. We therefore expect IRMOF-3-AM9, -AM13, -AM16, and -AM19 in particular to be extremely difficult, if not impossible, to prepare from solvothermal methods. Although only modified to a relatively small extent, these new MOFs are rather remarkable even from a structural standpoint. While it is relatively easy to incorporate long alkyl chains onto discrete metal−organic complexes,[66,67] it has proved extremely difficult to do so for their polymeric counterparts, and to the best of our knowledge, the new MOFs we have prepared herein represent the first examples of this family. The percent conversion for IRMOF-3-AM19 (~7%) suggests the modification is probably more than just on the surface,[68] although simple surface modification may be accessible via postsynthetic modification. Preliminary tests on IRMOF-3-AM19 samples show the MOF crystals are highly hydrophobic (float on an aqueous solution and aggregate, data not shown), indicating the successful grafting of hydrophobic substituents and at least some effective surface modification of the material.

**Porosity of Modified IRMOF-3.** From the perspective of a structure−function relationship, the physical and chemical properties of IRMOF-3 are expected to change upon modification by alkyl anhydrides. In particular, the systematic functionalization of IRMOF-3 with the 10 different reagents might be reflected by the overall porosity of the modified IRMOF-3 samples. Indeed, examination of the BET measurements of IRMOF-3-AM2 to -AM19 reveals an intriguing trend intimately associated with alkyl chain length. Our expectation was that the BET surface area would decrease as the alkyl chain length increased. To our surprise, when BET surface area is plotted versus alkyl chain length, a distinct "well-shaped" curve is observed, in which porosity of the MOF decreases from IRMOF-3-AM2 to -AM6 but increases from -AM7 to -AM19 (Figure 6). Indeed, IRMOF-3-AM3 and IRMOF-3-AM13 are found to possess comparable BET surfaces areas (1487 vs 1438 $m^2/g$), although the substituents in these two modified samples differ by 10 methylene groups. This perplexing result can be rational-

(66) Furukawa, H.; Kim, J.; Plass, K. E.; Yaghi, O. M. *J. Am. Chem. Soc.* **2006**, *128*, 8398–8399.
(67) Northrop, B. H.; Glöckner, A.; Stang, P. J. *J. Org. Chem.* **2008**, *73*, 1787–1794.
(68) Assuming the crystals have an idealized cubic shape with sides of length $l$, the total exposed surface area for each crystal would be $6 \times l^2$. A cubic unit cell on the other hand would have a surface area of $6 \times a^2$ ($a$ being the unit cell edge dimension). Because the total number of unit cells present in each crystal is $l^3/a^3$, the percent of exposed crystal surfaces vs total unit cell surfaces can be estimated to be $(6 \times l^2)/[(l^3/a^3)(6 \times a^2)] = a/l$. For a typical IRMOF-3 crystal ($l \approx 0.25$ mm; $a \approx 26$ Å), modification of only the crystal surface would give rise to a percent conversion far less than 1%.

***Table 4.*** Comparison of BET Surface Area and Determination of the Number of Additional Atoms (Excluding Hydrogen Atoms) Included per Cavity Due to Modification

| IRMOF-3 | -AM2 | -AM3 | -AM4 | -AM5 | -AM6 | -AM7 | -AM9 | -AM13 | -AM16 | -AM19 |
|---|---|---|---|---|---|---|---|---|---|---|
| *n* | 1 | 2 | 3 | 4 | 5 | 6 | 8 | 12 | 15 | 18 |
| no. of additional atoms per chain ($n + 3$)[a] | 4 | 5 | 6 | 7 | 8 | 9 | 11 | 15 | 18 | 21 |
| conversion (Table 1, Method 2) | 0.99 | 0.99 | 0.98 | 0.96 | 0.90 | 0.80 | 0.46 | 0.32 | 0.20 | 0.07 |
| no. of additional atoms per cavity[b] | 11.88 | 14.85 | 17.64 | 20.16 | 21.60 | 21.60 | 15.18 | 14.40 | 10.80 | 4.41 |
| BET surface area ($m^2/g$) | 1641 | 1487 | 1424 | 1201 | 1165 | 1185 | 1243 | 1438 | 1581 | 2164 |

[a] The number of atoms added per modified ligand were calculated by including one carbonyl oxygen, one carbonyl carbon, one methyl carbon, and *n* methylene carbons (only non-hydrogen atoms). [b] Obtained from the formula: ($n + 3$) × (conversion) × 3, where the second 3 is the number of unique amino groups per cavity, based on the empirical formula of $(Zn_4O)(NH_2-BDC)_3$.

ized on the basis of the actual number of atoms that are incorporated into each modified framework, noting that the degree of modification gradually decreases as the alkyl chain length increases. In fact, simple calculations taking into account both the percent conversion and the length of substituents suggest that surface areas of the modified MOFs correlate inversely with the number of additional atoms per unit volume and hence reasonably well with the effective free space available in the new MOFs (Table 4, Figure S32).

The apparent surface area of modified IRMOF-3 materials should intrinsically decrease when compared on a surface area per mass basis, because modification of the MOF necessarily increases the mass.[69] A more informative parameter may be the surface area per mole (Table S2), which should reveal changes in porosity, not simply related to increased mass, but rather related to changes in molecular structure of the pores. With this in mind, examination of the "molar surface area" of IRMOF-3 versus IRMOF-3-AM2 to IRMOF-3-AM19 (Figure S31) shows the same trend as that found in Figure 6. This strongly suggests that the observed decrease, then increase, in surface area of modified MOFs is not solely due to changes in mass but due to changes in the pore structure due to the presence of the acyl substituents. In this context, the concept of molar surface area, and thereby a means to compare the sorption capacity of an MOF on a per building unit basis, may have significant value in understanding changes in gas sorption at the molecular level.

The porosity of modified IRMOF-3 samples and the observation of a well-defined correlation between their surface areas and the alkyl chain length connote a number of significant implications in a broader context: (1) it corroborates the successful transformation of IRMOF-3 and suggests preservation of structural integrity of the modification products (i.e., microporosity); (2) it represents, to the best of our knowledge, the first systematic study in which the effects of covalent functionalization of MOFs are directly correlated to porosity; (3) it further confirms that the postsynthetic modification approach is a highly viable route to fine-tuning MOF architectures and their pore structures; and (4) it delineates a basic principle for the design of functionalized porous materials; i.e., the degree of functionalization and the level of porosity are mutually related. We therefore believe these general guidelines are not specific to the IRMOF-3 system but are of potential relevance for the development of a wider range of functional materials.

(69) The caveat to this assumption is that if a specific modification significantly increased sorption capacity (e.g., through stronger energetics of gas binding), then the anticipated drop in surface area would not necessarily be observed.

## Conclusions

As anticipated by Robson nearly 18 years ago, postsynthetic modification is a viable route toward preparing MOFs with new chemical and physical properties. Indeed, postsynthetic modification presents a systematic route for synthesizing functionalized MOFs with a high degree of control over the resulting products. The findings presented here indicate that the postsynthetic modification of MOFs is a versatile and general method for the functionalization of these important materials. IRMOF-3 has been postsynthetically modified using 10 alkyl anhydrides of increasing chain lengths. All 10 alkyl anhydrides successfully transformed IRMOF-3 to produce a range of IRMOFs that maintained the same crystallinity and thermal stability of as-synthesized IRMOF-3. A correlation between alkyl chain length and percent conversion was found (under fixed reaction conditions), where increasing alkyl chain length resulted in lower conversions. Reaction conditions were devised (Method 2) that achieved high conversions and generated high quality, modified products of suitable quality for single-crystal X-ray analysis that displayed high BET surface areas, consistent with retention of crystallinity and microporosity. More importantly, these studies show that MOFs can be modified to produce desired physical properties (i.e., hydrophobicity, resistance to water), without sacrificing porosity (e.g., IRMOF-3-AM19). Overall, these results confirm that postsynthetic modification is an efficient, versatile method for obtaining unprecedented MOFs with tunable functionality and novel physical properties.

**Acknowledgment.** We thank Dr. J. R. Stork for help with X-ray analyses, Prof. G. Arrhenius for use of his PXRD, and Dr. Y. Su for performing the mass spectrometry experiments. This work was supported by U.C.S.D., the donors of the ACS-PRF, and the NSF (CHE-0546531).

**Supporting Information Available:** Figures S1−S32, Tables S1 and S2. This material is available free of charge via the Internet at http://pubs.acs.org.

JA801848J